Springer

KSME

Journal of Mechanical Science and Technology 24 (12) (2010) 2511~2517
www.springerlink.com/content/1738-494x
DOI 10.1007/s12206-010-1003-2

Magnetic torque maximization in a camera shutter module by the topology optimization †

Jihun Kim[1], Kyung Ho Sun[2], Woochul Kim[3] and Jae Eun Kim[4,*]

[1]*Department of Mechanical Engineering, University of Michigan, Ann Arbor, MI 48105, USA*
[2]*School of Mechanical and Aerospace Engineering and National Creative Research Initiatives Center for Multiscale Design, Seoul National University, Seoul, 151-744, Korea*
[3]*Samsung Electronics Co., Ltd., Suwon Gyeonggi-Do 443-742, Korea*
[4]*Faculty of Mechanical and Automotive Engineering, Catholic University of Daegu, Geumnak 5-Ro, Hayang-Eup, Gyeongsan-Si, Gyeongbuk 712-702, Korea*

(Manuscript Received September 3, 2009; Revised May 2, 2010; Accepted August 17, 2010)

Abstract

In recent years, there has been a stronger demand for the weight reduction of components of various portable electronic devices. This work is motivated by the need to reduce the weight of a camera shutter module without much decreasing the torque generated by its magnetic circuit. Because the camera shutter speed is most significantly affected by the torque, the magnitude of the generated torque should also be considered in the design for the weight reduction. Thus, we formulate the design problem as a torque maximization problem under various mass constraints. Specifically, we propose to formulate it as a topology optimization problem of magnetic circuits and find optimal shapes of yokes (and magnets) in the circuits. For the maximization formulation, the objective function is chosen as the average of clockwise and counterclockwise torques over a whole range of rotation angles of a magnet corresponding to the shutter opening angle. Limits on the mass of the yoke and magnet in a magnetic circuit are imposed as constraints. The torque generated by a magnetic circuit is calculated by the modified Maxwell stress tensor method. A series of mass constraint ratios is considered to investigate the effects of the mass usage on the magnitude of torque generated by optimized circuits. The region occupied by the yoke (and the magnet) is designated as a design domain, while coils are assumed to belong to a non-design domain. By demonstrating that the optimized magnetic circuits outperform a nominal circuit, the use of the average torque as an objective function including a corresponding treatment of a rotating magnet proposed in this work is shown to be effective for the topology optimization of magnetic circuits in a camera shutter module.

Keywords: Camera shutter module; Magnetic torque maximization; Topology optimization; Weight reduction

1. Introduction

Many modern electronic portable devices, such as mobile phones and laptops, are equipped with camera modules for various reasons. Because lighter portable devices are preferred, the weight reduction of all components of a camera module including a shutter has become an important issue. This investigation is concerned with the weight reduction of a magnetic circuit in a camera shutter module.

For instance, a simple lightweight camera module consisting of an electromagnetic shutter driven by a magnetic torque [1] is shown in Fig. 1. In Fig. 1, the magnetic circuit of a camera shutter consists of a yoke, a coil, and a permanent magnet. When a current pulse is sent into the coil, the yoke is magnetized where the direction of the magnetic field depends on the sign of the current. If the magnetization directions in the yoke and the permanent magnet are misaligned, the camera shutter is opened due to the rotation of the permanent magnet by the magnetic attractive and repulsive forces. Since the performance of a camera module strongly depends on the shutter speed that controls the time period of light exposure, a magnetic circuit producing a faster shutter speed is desired, but the circuit mass should be minimized. To achieve both of these two goals, we formulate the design problem as a magnetic circuit topology optimization problem. The effectiveness of topology optimization for electromagnetic systems has been also demonstrated in earlier works [2-8]. Though there have been some investigations on the topology optimization of magnetic problems, no investigation has been reported on the topology optimization of a camera shutter.

In this work, the design problem is formulated as a torque maximization problem under various mass constraints. For the

† This paper was recommended for publication in revised form by Associate Editor Jeong Sam Han
* Corresponding author. Tel.: +82 53 850 2657, Fax.: +82 53 850 2710
E-mail address: jekim@cu.ac.kr

design optimization, the magnetic circuit is discretized with finite elements, and the magnetic torque is calculated by the modified Maxwell stress tensor method [9]. Because the magnetic torque affects the camera shutter speed most significantly, we propose to use the average magnetic torque over an operating range of rotation angles of the magnet as an objective function of the topology optimization problem. To investigate the dependence of the maximum torque value on a given mass usage, a series of torque maximization problems under various mass constraint ratios will be studied. Through these numerical studies, one can also determine the maximum weight reduction ratio relative to a nominal circuit without significantly reducing the magnitude of torque.

2. Topology optimization of magnetic circuits in a camera shutter module

2.1 Finite element analysis

To facilitate the topology optimization of the magnetic circuit, the finite element method in two-dimensional magnetostatic field is employed and the system matrix equation is given as follows:

$$\mathbf{K}\mathbf{A}_z = \mathbf{F}_{Magnet} + \mathbf{F}_{Coil}, \tag{1}$$

where $\mathbf{K}$ is the stiffness matrix associated with the magnetic degrees of freedom and $\mathbf{A}_z$ is the nodal magnetic vector potential in the z direction. The symbols $\mathbf{F}_{Magnet}$ and $\mathbf{F}_{Coil}$ denote the element load vectors resulting from magnets and coils, respectively. The matrices are explicitly given by the summation over the total number (n_e) of finite elements [10]:

$$\mathbf{K} = \sum_{e=1}^{n_e} \left\{ \frac{1}{\mu_e} \iint \left(\frac{\partial \mathbf{N}_e^T}{\partial x}\frac{\partial \mathbf{N}_e}{\partial x} + \frac{\partial \mathbf{N}_e^T}{\partial y}\frac{\partial \mathbf{N}_e}{\partial y} \right) dxdy \right\}, \tag{2}$$

$$\mathbf{F}_{Magnet} = \sum_{e=1}^{n_e} \left\{ \iint \left(H_{e,xc}\frac{\partial \mathbf{N}_e^T}{\partial y} - H_{e,yc}\frac{\partial \mathbf{N}_e^T}{\partial x} \right) dxdy \right\}, \tag{3}$$

$$\mathbf{F}_{Coil} = \sum_{e=1}^{n_e} \left(\iint J\mathbf{N}_e^T dxdy \right), \tag{4}$$

where μ_e denotes the magnetic permeability and $\mathbf{N}_e$ denotes the standard bilinear shape function. In Eq. (3), $H_{e,xc}$ and $H_{e,yc}$ denote the coercive force in the x and y directions, respectively. The symbol J denotes the volume current density. After $\mathbf{A}_z$ is determined, the magnetic flux density B in each direction is calculated as follows:

$$B_x = \frac{\partial \mathbf{N}_e}{\partial y}\mathbf{A}_z, \quad B_y = -\frac{\partial \mathbf{N}_e}{\partial x}\mathbf{A}_z. \tag{5}$$

2.2 Magnetic torque calculation

In the design of rotating machines, it is very important to calculate a magnetic torque fast and accurately. So far, the Maxwell stress tensor method [11] and the energy method [6, 7] have been used. However, these methods may not be the most effective in the application of topology optimization because a numerically calculated torque value may be affected by integration paths in the Maxwell stress tensor method, while a significant amount of computation is needed in the energy method using the finite element method. In this work, therefore, we employ the modified Maxwell stress tensor method [9]. It is based on the assumption that there are an infinite number of closed paths in the entire air gap and that the effect of the entire air gap elements on the generated magnetic torque can be considered by taking the average over an infinite number of the contours. Consequently, the magnetic torque calculated by this method is less dependent on the finite element discretization. Based on the modified method, the magnetic torque T is calculated by the following two-

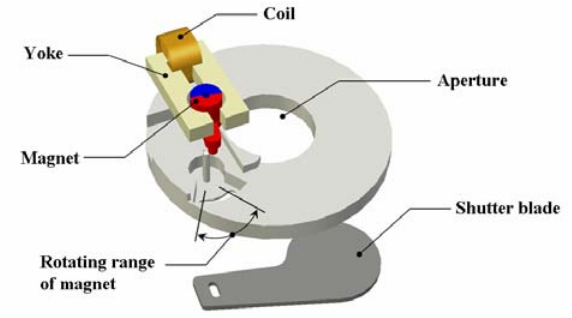

Fig. 1. Schematic description of a camera shutter device using a magnetic circuit.

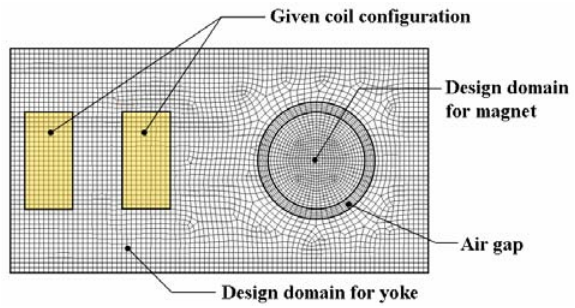

(a)

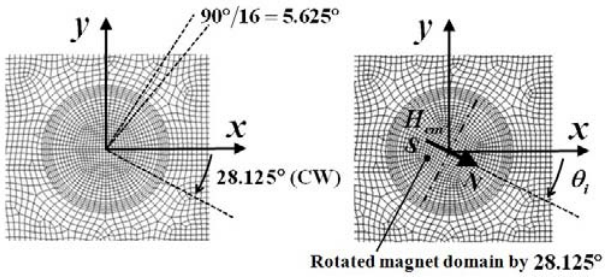

(b)

Fig. 2. (a) A two-dimensional magnetic circuit model used for optimization setup and (b) a finite element model of the permanent magnet before/after rotating with a corresponding coercive force shown.

dimensional area integration:

$$T = \frac{l}{\mu_0 g}\iint_S r B_t B_n dS\,, \tag{6}$$

where μ_0 is the permeability of air and g is the thickness of the air gap. In Eq. (6), l denotes the core depth and r denotes the distance from the axis of rotation to the integral path. The symbol S denotes the area of the air gap; B_t and B_n denote the tangential and normal components of the magnetic flux density, respectively. In this work, the magnetic torque in Eq. (6) is calculated by using an in-house code.

2.3 Optimization formulation

The design objective is to find an optimal magnetic circuit configuration consisting of the magnetic yoke and the permanent magnet that maximizes the magnetic torque for a given input current under various mass constraints. Fig. 2 shows a two-dimensional model used for the present optimization problem. One can compare Fig. 2 with the magnetic circuit of Fig. 1. Fig. 2 shows the yoke and magnet design domains discretized by finite elements. In setting up a topology optimization problem, two density design variables ρ_1 and ρ_2 are introduced for the yoke domain and the magnet domain, respectively. For the present camera shutter module, the following optimization setup is proposed:

Maximize

$$f = \frac{1}{(2N+1)}\left(\sum_{i=1}^{N}\left(\left|T_{\theta_i,ccw}\right| + \left|T_{\theta_i,cw}\right|\right) + \left|T_{\theta_i=0}\right|\right), \tag{7}$$

subject to

$$h_1(\rho_{e,1}) = \sum_{e=1}^{n_{yoke}} \rho_{e,1} v_{e,1} - M_{yoke} \le 0\,, \tag{8}$$

$$h_2(\rho_{e,2}) = \sum_{e=1}^{n_{magnet}} \rho_{e,2} v_{e,2} - M_{magnet} \le 0\,, \tag{9}$$

$$0 \le \rho_{e,1} \le 1 \quad (e = 1,\cdots,n_{yoke})\,, \tag{10}$$

$$0 \le \rho_{e,2} \le 1 \quad (e = 1,\cdots,n_{magnet})\,. \tag{11}$$

In Eq. (7), f denotes the average value of counterclockwise torques $T_{\theta_i,ccw}$ and clockwise torques $T_{\theta_i,cw}$ calculated at angles $\theta_i\ (i = 1,2,\ldots,N)$ by which the magnet is rotated about its own axis. In Eqs. (8)-(11), the symbols, n_{yoke} and n_{magnet}, denote the number of finite elements in the yoke and magnet domain, respectively. Therefore, Eqs. (8) and (9) state the constraints on the mass usage of the yoke and the magnet, respectively (M_{yoke} : given yoke mass, M_{magnet} : given magnet mass, $v_{e,1}$: mass of the e^{th} yoke, $v_{e,2}$: mass of the e^{th} magnet). Eqs. (10) and (11) denote the side constraints on the design variables.

Since the presence of a material in each element affects the permeability and the coercive force, an SIMP-like penalization technique (e.g., [12]) is adopted in this work as follows.

For yokes:

$$\mu_{e,1} = \mu_0\{1 + (\mu_{yoke} - 1)\rho_{e,1}^n\}\,. \tag{12}$$

For magnets:

$$\mu_{e,2} = \mu_0\{1 + (\mu_{magnet} - 1)\rho_{e,2}^n\}\,, \tag{13a}$$

$$H_{e,xc} = H_{xcm}\rho_{e,2}^n\,;\ H_{e,yc} = H_{ycm}\rho_{e,2}^n\,, \tag{13b}$$

where H_{xcm} and H_{ycm} denote the x and y components of the coercive force in the permanent magnet, respectively; n denotes the penalty exponent. According to Eqs. (12) and (13), material properties of the elements in the two design domains of yoke and magnet are stated as follows: if the design variable $\rho_{e,j}$ ($j = 1,2$) becomes zero, the element represents air. On the other hand, if the design variable is unity, the element represents either the yoke ($j = 1$) or the magnet ($j = 2$). In the magnet design domain, while an element with a zero value of design variable (air) has no coercive force, an element with a design variable equal to unity (permanent magnet) has a coercive force, which is dictated by Eq. (13b).

For the calculation of torques at each rotation angle, θ_i in Eq. (7), only the finite elements corresponding to the magnet design domain in Fig. 2 are rotated by the angle while the finite element model excluding the magnet domain always remains the same. Therefore, the components of the coercive force are also changed with the angle θ_i as follows (see Fig. 2(b) for the direction of the coercive force and the angle):

$$H_{xcm} = H_{cm}\cos\theta_i\,, \tag{14}$$

$$H_{ycm} = H_{cm}\sin\theta_i \ \text{(CCW)}, \tag{15a}$$

$$H_{ycm} = -H_{cm}\sin\theta_i \ \text{(CW)}, \tag{15b}$$

where H_{cm} denotes the coercive force in the permanent magnet. Each component of the penalized coercive force by using Eq. (13b) is then used in Eq. (3). In the procedure, the number of finite elements in the magnet domain in the circumferential direction determines the values of the angles, θ_i . In Fig. 2(b), since the number of finite elements in the first quadrant is 16 and 90º/16=5.625º, the rotation angles of the magnet domain are selected among integral multiples of 5.625º for the element connectivity between the magnet domain and the air gap.

For the sensitivity analysis, the adjoint variable method is employed [13].

$$L = f + \boldsymbol{\lambda}^T(\mathbf{F}_{Magnet} + \mathbf{F}_{Coil} - \mathbf{K}\mathbf{A}_z)\,, \tag{16}$$

where L denotes the augmented objective function and λ denotes the adjoint variable vector. After differentiating Eq. (16) with respect to the design variable, we obtain

$$\begin{aligned}\frac{dL}{d\rho_{e,j}} &= \frac{\partial f}{\partial \rho_{e,j}} + \frac{\partial f}{\partial \mathbf{A}}\frac{d\mathbf{A}}{d\rho_{e,j}} + \boldsymbol{\lambda}^T \frac{\partial}{\partial \rho_{e,j}}(\mathbf{F}_{Magnet} + \mathbf{F}_{Coil}) \\ &\quad - \boldsymbol{\lambda}^T \frac{\partial \mathbf{K}}{\partial \rho_{e,j}}\mathbf{A} - \boldsymbol{\lambda}^T \mathbf{K}\frac{d\mathbf{A}}{d\rho_{e,j}} \\ &= \frac{\partial f}{\partial \rho_{e,j}} + \boldsymbol{\lambda}^T \frac{\partial}{\partial \rho_{e,j}}(\mathbf{F}_{Magnet} + \mathbf{F}_{Coil}) \\ &\quad - \boldsymbol{\lambda}^T \frac{\partial \mathbf{K}}{\partial \rho_{e,j}}\mathbf{A} + \left(\frac{\partial f}{\partial \mathbf{A}} - \boldsymbol{\lambda}^T \mathbf{K}\right)\frac{d\mathbf{A}}{d\rho_{e,j}}.\end{aligned} \tag{17}$$

From the above equation, the adjoint variable is calculated by solving the following equation

$$\mathbf{K}\boldsymbol{\lambda} = \frac{\partial f}{\partial \mathbf{A}_z}, \tag{18}$$

which is obtained by setting the last term in Eq. (17) equal to zero. Therefore, the sensitivities of the objective function with respect to each design variable are calculated by

$$\frac{dL}{d\rho_{e,1}} = \frac{\partial f}{\partial \rho_{e,1}} - \boldsymbol{\lambda}^T \frac{\partial \mathbf{K}}{\partial \rho_{e,1}}\mathbf{A}, \tag{19}$$

$$\begin{aligned}\frac{dL}{d\rho_{e,2}} &= \frac{\partial f}{\partial \rho_{e,2}} \\ &\quad + \boldsymbol{\lambda}^T \frac{\partial}{\partial \rho_{e,2}}(\mathbf{F}_{Magnet} + \mathbf{F}_{Coil}) - \boldsymbol{\lambda}^T \frac{\partial \mathbf{K}}{\partial \rho_{e,2}}\mathbf{A}.\end{aligned} \tag{20}$$

In Eq. (19), the derivative of the load matrix, $\mathbf{F}_{Magnet}$ or $\mathbf{F}_{Coil}$, with respect to the design variable becomes zero because the load matrix is independent of the design variables assigned to the yoke design domain.

For the proposed topology optimization of magnetic circuits in a camera shutter module, the total number of analyses in one iteration of optimization is $2\times(2N+1)$, $2N+1$ for the response analysis and $2N+1$ for the sensitivity analysis, respectively.

3. Numerical results

Before we find an optimized magnetic circuit by using Eqs. (7)-(20), we introduce the magnetic circuit proposed in [1] as a nominal circuit. A nominal circuit configuration employed is shown in Fig. 3; specifically, it is assumed that the nominal yoke fills 57.4% of the given yoke design domain and the nominal magnet, 100% of the given magnet design domain shown in Fig. 2. For the optimization, the numerical data used are as follows:

- air permeability: $\mu_0 = 4\pi\times10^{-7}$ H/m
- relative permeability of the yoke: $\mu_{yoke} = 1000$
- relative permeability of the magnet: $\mu_{magnet} = 1.13$
- coercive force: $H_{cm} = 70000$ A/m
- volume current density: $J = 2\times10^8$ A/m^2
- number of angles used for torque calculation: $N = 5$

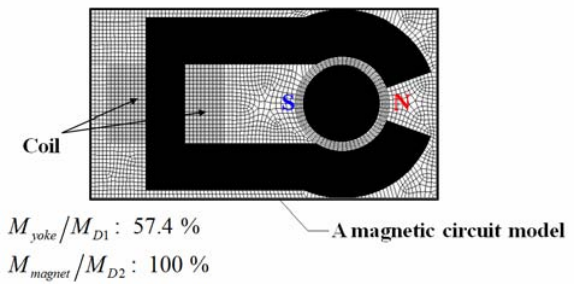

Fig. 3. A nominal magnetic circuit colored in black. The symbols M_{D1} and M_{D2} denote the total masses of the yoke and magnet design domains while M_{yoke} and M_{magnet}, the corresponding masses of a nominal magnetic circuit.

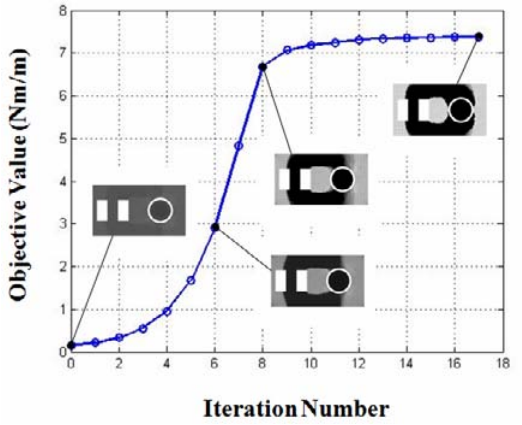

(a)

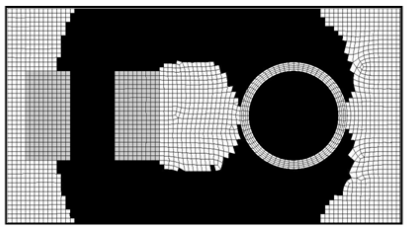

(b)

Fig. 4. (a) The optimization iteration history and (b) the optimized configuration under the same mass usage as that for the nominal case shown in Fig. 3.

- rotation angle range of the magnet in consideration: $-30° \le \theta \le 30°$
- numbers of finite elements in the design domain: $n_{yoke} = 3200$, $n_{magnet} = 768$
- penalty exponent: $n = 3$

For a gradient-based optimization algorithm, the method of moving asymptotes (MMA) [14] is used in this work.

As the first design problem, we find an optimized yoke in the magnetic circuit under exactly the same mass ratio as the nominal circuit. Fig. 4(a) shows the iteration history of the objective function, i.e., the averaged magnetic torque. The finally optimized result is also shown in Fig. 4(b). Uniform

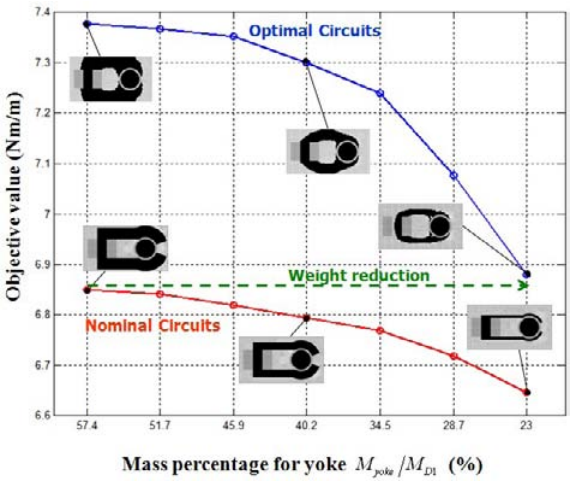

Fig. 5. Comparison between the nominal circuits and the optimized circuits under various constraints.

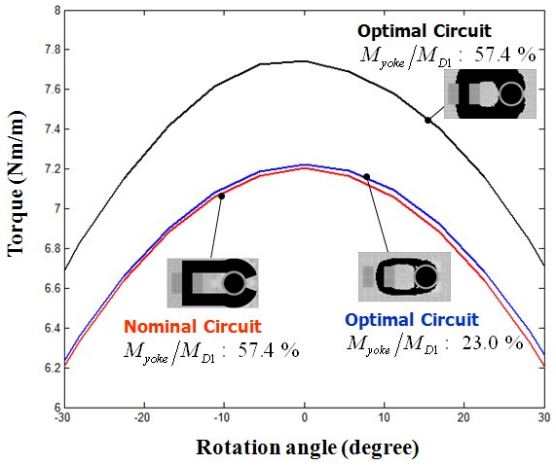

Fig. 6. Comparison of the magnetic torques over the operating of angle between the nominal and optimal circuits.

convergence is demonstrated from Fig. 4(a) and convergence to a distinct yoke-air distribution is apparent from Fig. 4(b), which is obtained by using a threshold value of 0.5, i.e., $\rho_{e,1}=0$ for $\rho_{e,1}<0.5$ and $\rho_{e,1}=1$ for $\rho_{e,1}\geq 0.5$.

After checking the convergence behavior by the developed formulation, the effects of the mass usage on the magnitude of torque generated by optimized magnetic circuits will be now investigated. Fig. 5 compares the objective function values of the nominal and optimized magnetic circuits as the allowed mass usage is decreased. To compare the optimized results with the nominal ones, the permanent magnet was not considered as a design domain (i.e., $M_{magnet}/M_{D2}=100\%$). From this investigation, while the improvement in the average torque is about 8% for the optimized circuit subject to the same mass usage of yoke as the nominal one, one can see that the topology optimization can reduce the weight of the yoke by more than 30% without any decrease in the objective function value.

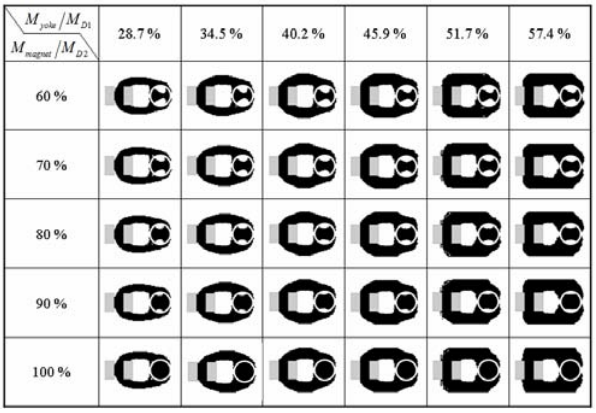

Fig. 7. The optimized magnetic circuits obtained under the mass combinations of M_{yoke}/M_{D1} and M_{magnet}/M_{D2}.

The magnitudes of magnetic torque over the whole range of operation are shown in Fig. 6, where the three cases of the nominal model, the optimized model with the same mass usage of yoke as the nominal one, and the model optimized to have a similar objective value to the nominal one are compared. The graph is plotted by connecting the values at 0º, 5.625º, 11.25º, 16.875º, 22.5º, 28.125º, 33.75º. It clearly shows that the maximization of generated torques at each angle within a range of operation can be achieved by the proposed objective function in the form of the average torque.

Fig. 7 shows the optimal magnetic circuits obtained under various combinations of yoke and magnet mass ratios. From Fig. 7, one can observe a certain pattern in the optimized shapes of the yoke and magnet as the mass ratios decrease. This pattern helps magnetic circuit designers find optimal yoke/magnet shapes of the magnetic circuit in camera shutter modules. In Fig. 8, the objective function values of the optimized magnetic circuits in Fig. 7 are plotted with respect to the mass usage of both yoke and magnet. This graph shows that the objective function has uni-modal properties for the mass usages of both the yoke and magnet, which means that its value increases as the mass usage increases. In addition, as the mass usage decreases, the decrement rate of the objective function value increases. Based on this observation, one can infer that there exists a certain value of the mass usage for the yoke and magnet without significantly reducing the magnitude of torque.

To show the effectiveness of the proposed objective function and the corresponding treatment of the magnet design domain, they are also applied to the case where the vertical dimension of the yoke design domain is increased. From the optimized circuit in Fig. 4 subject to the same amount of mass usage as that for the nominal design, it seems that the yoke design domain is rather restricted. The optimized results in Fig. 9 are obtained with the vertical dimension of the yoke design domain doubled, where no threshold for the design variable is used. The amounts of mass usage (M_{yoke}/M_{D1}) for the yoke are set as 57.4% and 114.8 %, respectively, where the value of

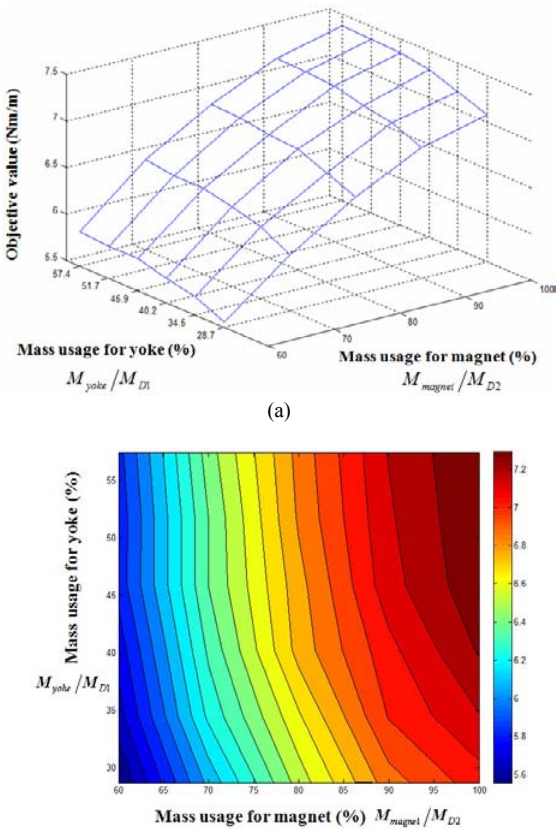

Fig. 8. (a) The surface plot for the objective values of the magnetic circuits versus the mass usages of the yoke and magnet and (b) their contour plot.

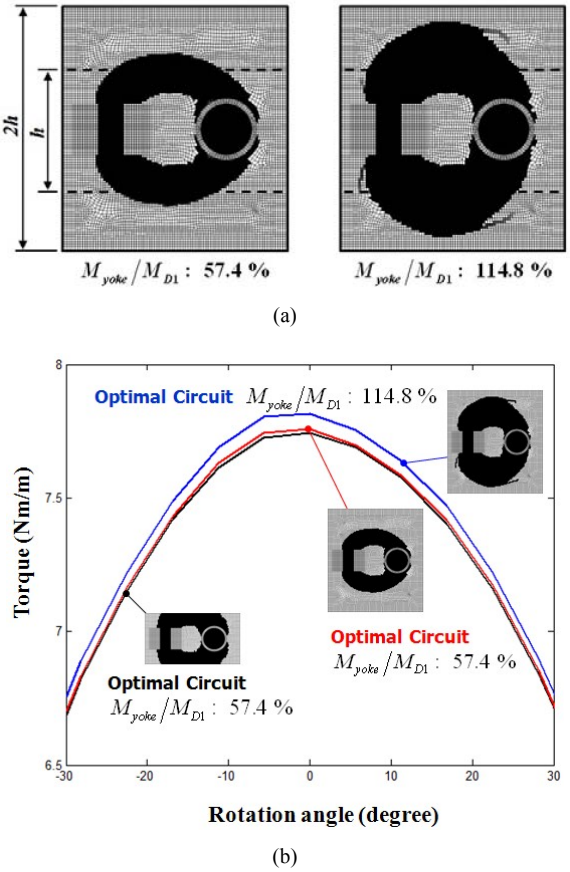

Fig. 9. (a) The optimized results for the yoke design domain with increased dimension in the vertical direction and (b) the comparison of the magnetic torques.

M_{D1} is calculated with respect to the yoke design domain in Fig. 2. As shown in Fig. 9(b), although the improvement in the magnitude of torque is not significant, it can be observed that the material distribution is more vertically oriented.

4. Conclusions

The mass reduction of a magnetic circuit without deteriorating its magnetic torque in a camera shutter module was formulated and solved as a magnetic circuit topology optimization problem. For the formulation, the objective function was chosen to be the average torque over a complete period of clockwise and counterclockwise shutter motions and the constraint, to be a given amount of the magnetic circuit mass. After checking the validity of the developed formulation, we systematically investigated the effects of the mass usage on the optimized shapes of the yoke and the magnet. Some interesting findings from this investigation are as follows: i) when the mass constraint on the magnet is tight, the optimized magnet shape is considerably different from the nominal circular shape, and ii) on the other hand, the optimized yoke shape is only slightly different from the nominal yoke, even when the mass constraint on the yoke is tight. Through this investigation, the effectiveness of the developed topology optimization formulation for magnetic torque problems in a camera shutter module was demonstrated and the effects of the mass of the magnetic circuit on the optimized results were understood.

Acknowledgment

This research was supported by the National Creative Research Initiatives Program (Korea Research Foundation Grant No. 2010-0019241) contracted through the Institute of Advanced Machinery and Design at Seoul National University and by the WCU (World Class University) program (Grant No. R31-2009-000-10083-0) through the Korea Research Foundation funded by the Ministry of Education, Science, and Technology. The authors also would like to thank Professor Yoon Young Kim at School of Mechanical and Aerospace Engineering, Seoul National University for his advice and support.

References

[1] J. Jung, K. T. Lee, M. H. Lee, S. Hong and E. Ko, Camera module actuator and electromechanical shutter for mobile phone, *Proc. of the Korean Society for Noise and Vibration Engineering Annual Autumn Conference* (2005) 740-743.

[2] D. N. Dyck and D. A. Lowther, Automated design of magnetic devices by optimizing material distribution, *IEEE Trans. Magn.,* 32 (1996) 1188-1193.
[3] W. Kim and Y. Y. Kim, Design of a bias magnetic system of a magnetostrictive sensor for flexural wave measurement, *IEEE Trans. Magn.,* 40 (2004) 3331-3338.
[4] W. Kim, J. E. Kim and Y. Y. Kim, Coil configuration design for the Lorentz force maximization by the topology optimization method: applications to optical pickup coil design, *Sens. Actuators A-Phys.,* 121 (2005) 221-229.
[5] J. Yoo, Reduction of vibration caused by magnetic force in a switched reluctance motor by topology optimization, *J. Appl. Mech.*, 69 (2002) 380-387.
[6] J. Byun and S. Hahn, Application of topology optimization to electromagnetic system, *Int. J. Appl. Electrom. Mech.*, 13 (2001) 25-33.
[7] S. Wang, J. Kang and J. Noh, Topology optimization of a single-phase induction motor for rotary compressor, *IEEE Trans. Magn.*, 40 (2004) 1591-1596.
[8] S. Wang, D. Youn, H. Moon and J. Kang, Topology optimization of electromagnetic systems considering magnetization direction, *IEEE Trans. Magn.*, 41 (2005) 1808-1811.
[9] L. Chang, A. R. Eastham and G. E. Dawson, Permanent magnet synchronous motor: finite element torque calculations, *Proc. of IEEE IAS Annu. Meeting*, 1 (1989) 69-73.
[10] S. J. Salon, *Finite Element Analysis of Electrical Machines*, Kluwer Academic Publishers, New York (1995) 35-39.
[11] E. S. Hamdi, *Design of Small Electrical Machines*, Wiley, New York (1994).
[12] M. P. Bendsøe and O. Sigmund, Material interpolation schemes in topology optimization, *Arch. Appl. Mech*., 69 (1999) 635-654.
[13] K. K. Choi and N. Kim, *Structural Sensitivity Analysis and Optimization 1: Linear Systems*, Springer, New York (2004).
[14] K. Svanberg, The method of moving asymptotes: a new model for structural optimization, *Int. J. Numer. Meth. Eng*., 24 (1987) 359-373.

Jihun Kim is pursuing his Ph.D. degree in Mechanical Engineering at the University of Michigan, Ann Arbor, USA. His current research involves finite element method-based deformable image registration on intensity-modulated radiation therapy. He received his Bachelor's and Master's degrees in Mechanical Engineering at Seoul National University, Korea in 2006 and 2008.

Jae Eun Kim received his Ph.D. in Mechanical Engineering at Seoul National University, Korea, in 2005. He worked at LG electronics as a senior/chief engineer in an actuator developing department and then at National Creative Research Initiatives Center as a senior research engineer in Seoul National University. He works in the Faculty of Mechanical and Automotive Engineering of Catholic University of Daegu, Korea. His main research interest is the design of multiphysics systems focused on the wave and vibration phenomena.